

Development of imaging bolometers for long-pulse MFE experiments (invited)

G. A. Wurden and B. J. Peterson^{a)}

Los Alamos National Laboratory (LANL), Los Alamos, New Mexico 87545

(Presented on 8 June 1998)

We have developed the concept of an imaging bolometer, capable of operation with 100's of individual channels, while relying on optical (infrared) readout of the temperature rise in a thin foil. A thin gold foil (0.5–5 μm thick) is sandwiched between pieces of copper. The copper mask (a large thermal mass) has a hole pattern drilled into it to form many "individual pixels," effectively forming many separate sensors. This segmented foil/mask combination is exposed on its front side to plasma radiation through a cooled pinhole camera geometry. Simultaneously, a high-resolution infrared camera monitors any temperature change on the backside of the thin foil. A sensitive infrared (IR) camera views the foil through an IR telescope/periscope system, and is shielded from the magnetic and nuclear radiation fields, either by distance and/or material shielding. A simple time-dependent design algorithm, using 1D heat transport to a cold boundary, has been written in MathCad, which allows us to select optimal material and geometries to match the expected plasma conditions. We have built a compact prototype with 149 channels, and tested it successfully both in a vacuum test stand in the laboratory, and on a plasma in the CHS at the National Institute for Fusion Science, subjecting it to electron cyclotron heated and neutral beam injection heated conditions. A water-cooled version has been built for the new LHD. Since the IR imaging bolometer uses only metal parts near the plasma, and has no need for wiring or wiring feedthrus, it is intrinsically radiation hard, and has direct application to ignition device to test engineering concepts (ITER), or ITER-class experiments. © 1999 American Institute of Physics. [S0034-6748(99)66101-9]

I. INTRODUCTION

We desire to measure the total energy loss from the plasma with good spatial and temporal resolution. Generally, this includes radiation and energy carried by particles. Usually, the two loss mechanisms are considered together, and separate techniques must be used if it is desired to discriminate between the two loss channels. For the moment, we consider the two together, if the detector responds to both in a similar fashion. In order to measure the total radiation from the plasma, a wide-band radiation detector is required. To the extent that a metal foil (with a known heat capacity and thermal response function) can act as a broadband absorber of impinging radiation, one can measure the temperature rise in the foil to infer the incident energy on the foil as a function of time.¹ A Joint European Torus (JET) or Tokamak Fusion Test Reactor (TFTR)-type bolometer² does this by monitoring the change in resistance of a resistive element with temperature, with the resistor being thermally bonded to the absorbing element. In a related fashion, a pyroelectric bolometer monitors a voltage that is produced by a temperature change in a pyroelectric material. So-called "silicon extreme ultraviolet (XUV) bolometers" do not rely on a temperature rise, but instead use semiconductor effects to allow photons to directly generate electrical currents, without the conversion to heat.

^{a)}Also at: National Institute for Fusion Science (NIFS), Toki-shi, Japan.

Bolometers are "old" diagnostics. Their use in plasma fusion experiments is well developed.³ However, due to a number of issues associated with the next generation of magnetic fusion devices and new technologies that have arisen in the last 10 years, we have taken a new look at the whole issue of optimizing bolometers for applications involving complex-shaped, steady state, plasmas. This article summarizes a three-year collaborative effort on the part of Los Alamos National Laboratory (LANL) and National Institute for Fusion Science (NIFS) to develop an infrared readout imaging bolometer, which can be used to observe a steady state, high temperature, fusion-grade plasma. Results are reported from instruments that have been constructed and tested, both in the laboratory, and on the compact helical stellarator (CHS) plasma device.

II. DESIGN

As with any plasma diagnostic, the design of a bolometer system is subject to many constraints, as shown in Table I. The infrared imaging bolometer concept trades-off and solves some of these issues in an interesting fashion. The first single detector infrared bolometers were developed for TFR tokamak and ZT-40 reversed field pinch machines nearly 15–20 years ago.⁴ At that time, it was recognized that they are not as sensitive as direct "resistive" bolometric measurements, but were useful in the case of a noisy environment because of superior electrical isolation due to the optical readout.

TABLE I. Generic diagnostic design issues.

Issues for diagnostic design.
1. Required sensitivity and precision
2. Achievable spatial resolution
3. Achievable time resolution
3. Access to the plasma
4. Radiation-hardness
5. Sources of noise/interference
6. What other parameters are required for data interpretation?
7. Data handling
8. Reliability
9. Ease of maintenance
10. Cost and cost/channel

Because a bolometer must directly view the plasma (no mirrors work for all wavelengths of light), it must be in vacuum, near the first wall of the plasma. Depending on the power fluxes to the first wall, the power to the bolometer sensor can be controlled by a judicious use of apertures and geometry. The achievable field of view, the plasma geometry, and the number of viewing positions necessary to unfold the source distribution, all are tied together. The collimation of individual “channels” or pixels in the detector, with the resulting reduction of power across many individual detector elements has to be balanced within the context of the expected power densities on the one hand, and the minimum detectable signal level on the other, while being limited by the desired time resolution (integration times). When you solve this generic problem for one channel, including getting the data out of the vacuum via some technique (wiring and feedthrus, or by using mirrors), you still are not done. The complexity, reliability, and additional costs of multiplying by dozens, or even thousands of discrete signals must be considered.

We have reported the design of an imaging IR bolometer in a previous paper.⁵ Since then, we have actually built prototype instruments⁶ and encountered several additional issues.

A key issue for efficient and accurate readout of the foil temperature by optical means, is that the emissivity of the side of the foil which faces the infrared camera, must be as close to unity as possible. Pure gold foil is of course an excellent infrared mirror (emissivity $\epsilon \sim 0.01$), and is unsuited to this task by itself. We have used a commercially available graphite spray called “Aerodag” (“containing micron-sized graphite particles” from an American company named Acheson Colloids in Port Huron, Michigan), to blacken the surface of the gold foil. The measured emissivity in the wavelength range of 3–5 and 8–12 μm is $\epsilon = 0.95$. We spray on as little as possible (just enough to make the gold appear black to the human eye). In a materials characterization lab at LANL we have measured the absorption of gold M lines to K line soft x-ray emission from a sample blackened gold foil, and with modeling have determined that the graphite thickness is equivalent to $\sim 0.2\text{--}0.4 \mu\text{m}$ of solid graphite. A scanning electron micrograph of the graphite coating is shown in Fig. 1. The surface is very rough, look-

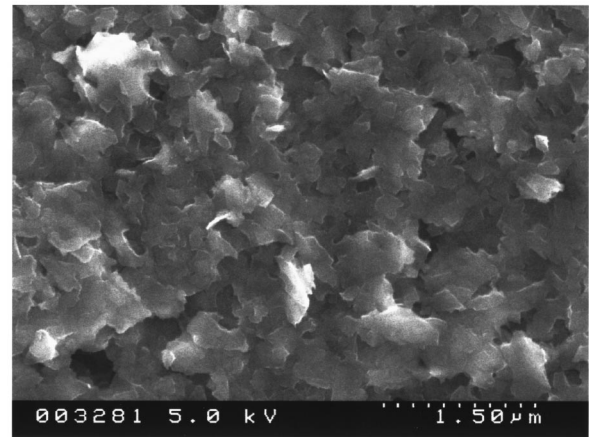


FIG. 1. Scanning electron microscope picture of the black (graphite) coating, deposited by “Aerodag” spray on the thin gold foil. The graphite flakes are submicron in size.

ing like corn flakes spilled on a flat surface. Due to possible nonuniformities in the foil thickness, blackening, or assembly of a foil/mask combination, it is still necessary to calibrate each and every pixel in the array. To the extent that the propagation of heat into the foil thickness takes only a very short time compared to the radial cooling of the pixel, then the radiated power P_{rad} at each pixel can be approximated by

$$P_{\text{rad}}(t) = \frac{1}{K} \left(T(t) + \tau_c \frac{dT(t)}{dt} \right),$$

where K is a calibration factor (in our case, for example, $^{\circ}\text{C}/\text{mW}$), τ_c is the cooling time constant of the pixel, and $T(t)$ is some measure of the foil temperature (peak, or spatially averaged, for example) as a function of time. Both coefficients can be measured by using a He–Ne laser to put a known power onto the blackened pixel (giving us K in steady state), and then by observing the exponential decay of the temperature when the laser beam is suddenly blocked to obtain τ_c . In principle, these two parameters could be applied for each pixel in the array in real time, using a digital signal processor, but we have not demonstrated this in the laboratory yet.

III. LAB TEST RESULTS

In order to test a bolometer in the laboratory, you need a source of “radiation,” and a vacuum. Of course, the best calibration source would be a plasma with the same energy spectrum of radiation that you ultimately want to measure. Generally, however, this is not readily available. As a substitute, either resistive heating of the foil, or laser deposition of a known amount of energy/power is used instead. In either case, a separate measure of the reflectivity of the absorbing material comprising the first surface of the bolometer is required. A further requirement to test the bolometer in vacuum is absolutely essential, because air acts as an additional heat transport channel on the bolometer foil that is usually not present in fusion plasma operating scenarios. In this regard, it has been already noted in large tokamaks that under some conditions, large fluxes of neutrals (either near a

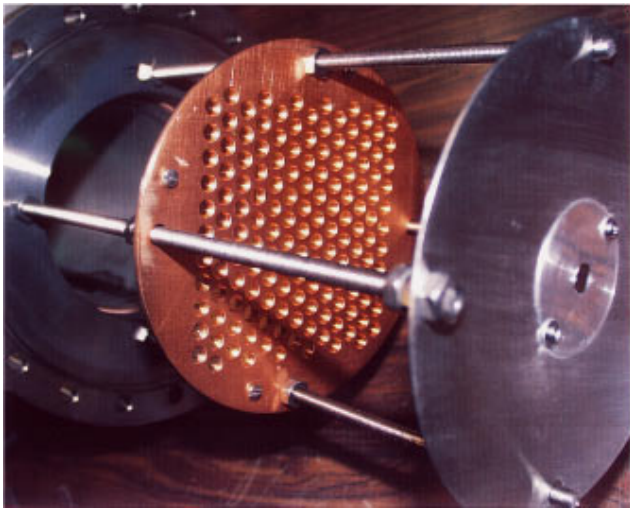


FIG. 2. Foil/mask is mounted behind a simple 8 mm diameter pinhole, before being inserted into a close-fitting port.

gas puff valve, or when viewing through a divertor, or during late stages of a disruption) can alter the interpretation of bolometer signals.

We have tested foil/mask combinations with individual pixels ranging from 3 to 10 mm in diameter. The number of pixels range from 6×6 to 12×13 in each mask, limited by port constraints and spatial resolution of our infrared cameras and lenses, although we envision arrays of up to 30×30 elements may be practical with today's technologies. Figure 2 shows a 149-element foil/mask, which views the plasma through the pinhole on the right. By steering a focused He-Ne laser to the backside of each pixel, one could map the response of all 149 elements, individually. We are planning to program a powerful "grocery-store laser scanner"

(or something equivalent) to do the job automatically. The experimentally measured thermal decay times of our pixels are routinely 2–3× longer than what our simple Bessel function MathCad model⁵ would predict for pure gold foils. We believe that this is due to effects of the graphite coating, and possible imperfect thermal contact between the foil and copper mask. In the future, a better clamping scheme will be employed in the foil/mask assembly to overcome this problem.

IV. EXPERIMENTS AT CHS

In order to test the IR bolometer with a real plasma, we have chosen to experiment on the CHS stellarator plasma at the NIFS Nagoya University site.⁷ This toroidal plasma has substantial auxiliary heating, is readily accessible, has short lead times to mount hardware, good access, and has a well-characterized range of plasma conditions. In 1997 it also served as a test bed for standard "PTS" bolometers⁸ which are now used on large helical device (LHD). It also has realistic sources of noise, including ECRH and neutral beam high voltage supplies, and rapidly changing magnetic fields. However, it has a relatively short pulse length (~100 ms), and of course, no significant nuclear radiation problem. Typically, the plasma is initiated with a 20 ms, 200 kW burst of 53 GHz electron cyclotron resonance heating (ECH). Then a neutral beam (~900 kW) is applied to the ECH target plasma, and the pulse is extended for another 100 ms. A typical set of wave forms during our experiments is shown in Fig. 3. From the point of view of our bolometry tests, it is important to look at the radiated power signal from a wide-angle pyro-bolometer (dashed line in the second wave form), which is of order 150–200 kW, depending on the amount of titanium gettering and wall conditions.

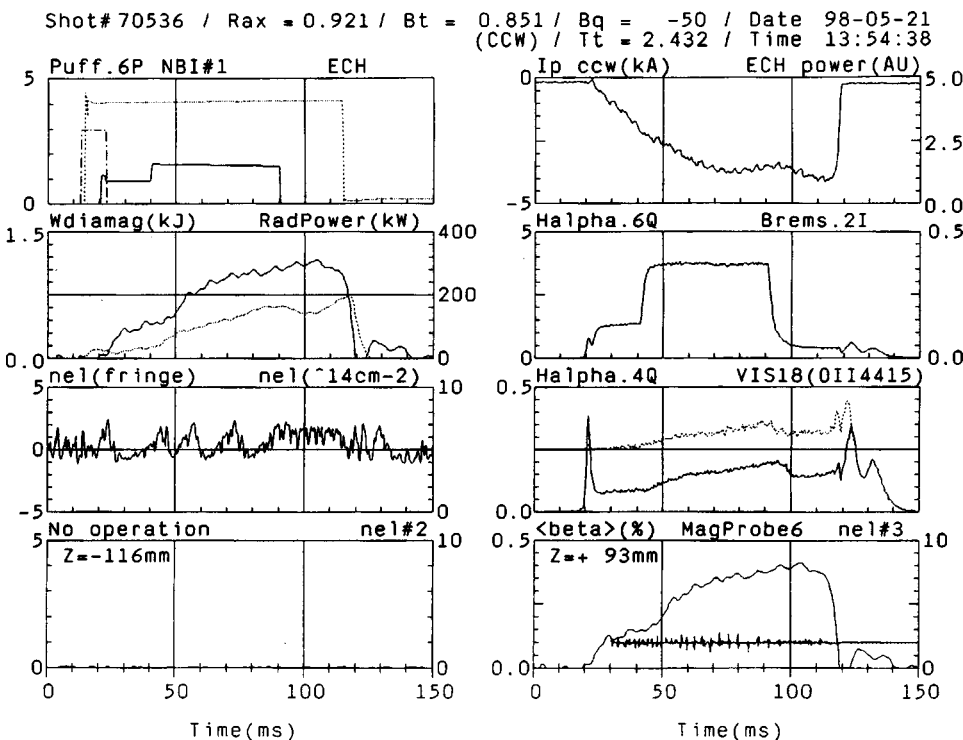


FIG. 3. Typical CHS waveforms during the IR bolometer tests in May 1998, shot 70536, showing ECH NBI, and gas puff timing pulses, diamagnetic stored energy and radiated power, plasma interferometer, induced toroidal current (by NBI), H alpha light, H alpha and OII light, plasma beta and Mirnov activity. The radiated power is ~100–200 kW.

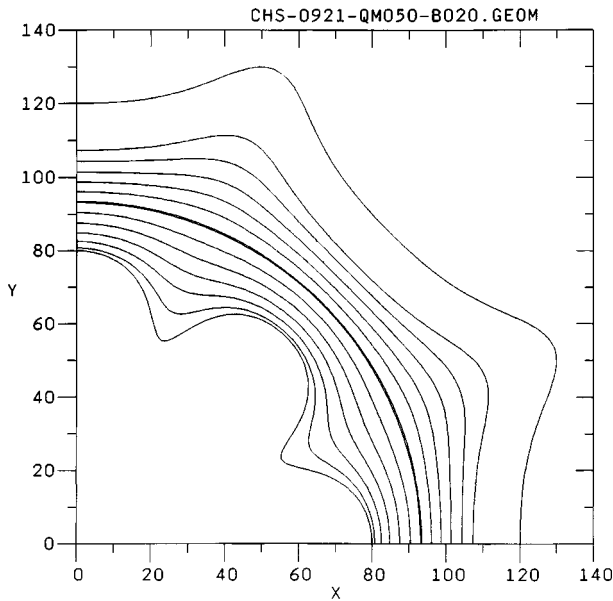


FIG. 4. One-quarter section of CHS magnetic surfaces, viewed from above, calculated for a 0.2% beta plasma positioned at a major radius of 92.1 cm. The IR Bolometer images the plasma from a major radius of 94 cm, looking upwards in a port located at a “narrow” section of the plasma. Dimensions are shown in centimeters.

The helical stellarator configuration is a particularly interesting target plasma on which to employ 2D imaging bolometry, because of its somewhat complicated plasma shape. The plasma poloidal cross section is basically an ellipse, with x points at the narrow ends of the ellipse, and the ellipse rotates poloidally as you go around the machine in the toroidal direction. A top-view diagram of the magnetic surfaces for a plasma centered at 92.1 cm major radius, assuming 0.2% beta, is shown in Fig. 4. Our bolometer views the plasma looking straight up from a port located underneath

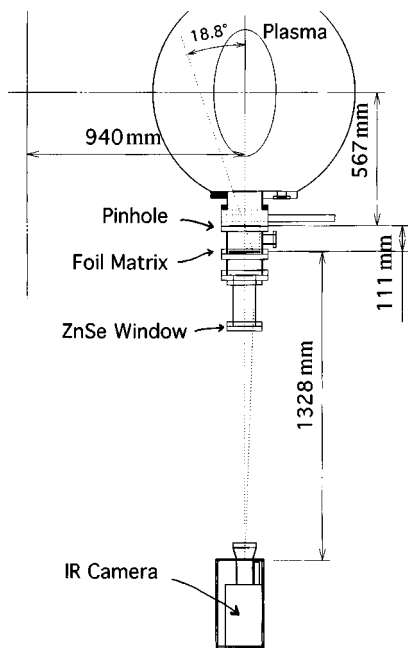


FIG. 5. Side-view schematic layout of the IR Bolometer on CHS.

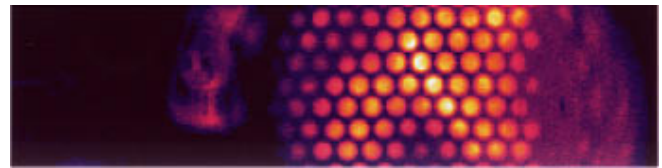


FIG. 6. One frame of a 30 Hz IR bolometric image taken with the Agema camera on CHS. The major radius direction is horizontal. Toroidal direction is vertical.

the machine, at a “narrow” position of the plasma, at 94 cm major radius. If the plasma radiation is uniform, then the imaging bolometer should see a narrow plasma when viewing straight up, while becoming wider (radially) as you look in either direction toroidally. Alternatively, if the radiation is concentrated near the “ x -point” tips, then the imaging bolometer should see an “ X ” pattern due to the rotation of the ellipse in either direction as you move toroidally. The opening angle (field of view) of our test pinhole camera arrangement is limited by a port aperture to $\sim \pm 19^\circ$. The layout is shown schematically in Fig. 5.

The magnitude of signals (a few $^\circ\text{C}$) was approximately what we expected. However, an interesting pattern was seen in both radial and toroidal directions, during CHS shots which were formed by a vertical launch ECH antenna (this means, most CHS discharges). An example is shown in Fig. 6, which is one frame of a 30 Hz infrared image during CHS shot 70378. Unfortunately, most of this image ($\sim 2/3$ of it) turns out to be caused by ECH “pickup,” and not true plasma radiation. The horizontal direction corresponds to the radial direction. The full plasma cross section, from inside to outside is covered. The outside of the plasma major radius is to the right. The signal is from the part of the image with the “honeycomb” pattern. The round feature on the left is part of a Conflat flange, and is not relevant. This image is not corrected for differing relative sensitivities or differing decay time constants, which would be necessary to give a true image. To do this requires pixel-by-pixel calibration as mentioned above. Faster time response can be achieved by

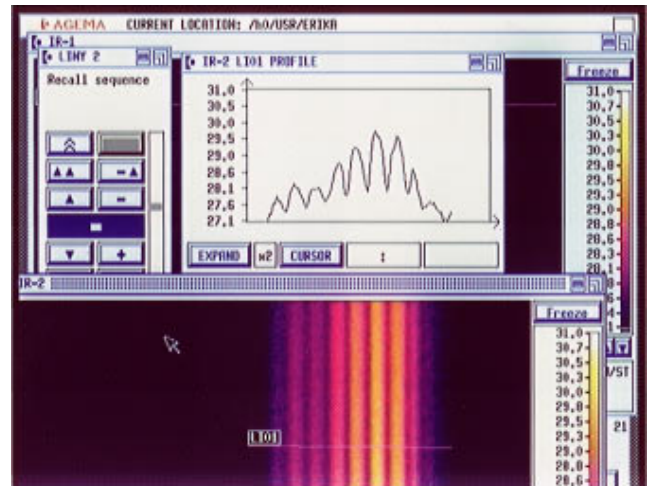


FIG. 7. Screen snapshot of the Agema control computer, showing a replay of a fast linescan. The camera reads out in $^\circ\text{C}$, and a spatial lineout is plotted across one row of pixels (at one time).

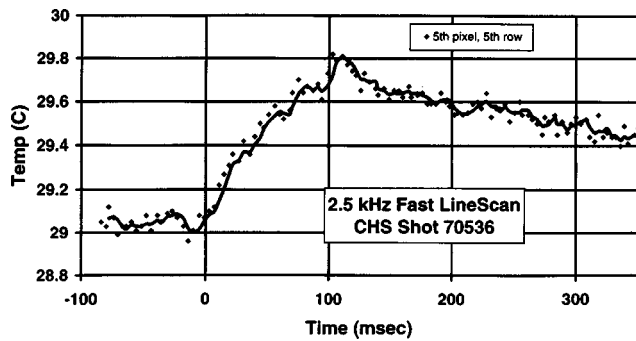


FIG. 8. Fast line scan, lineout of one pixel during a shot with no ECH interference. Corresponding plasma parameters are shown in Fig. 3.

switching to the 2.5 kHz fast linescan mode (~ 80 millidegrees K sensitivity) of the Agema infrared camera, and then taking slices across each row, on a shot-by-shot basis. A screen snapshot from a similar discharge (70364) using a fast linescan is shown in Fig. 7. The image is similar to that from a streak camera (space horizontal, and time axis is vertical). The 12-bit digital data can be scrolled through the entire shot, and quantitative temperature versus time plots from any “pixel” can be made. Finally, in Fig. 8, this type of data from one pixel is shown from a shot where an ECH launcher on the opposite side of the machine (across from where the IR Bolo was located) was used to initiate the plasma. In this case, almost the entire signal is in fact due to plasma radiation (and not due to ECH pickup). The heating power switched off at 110 ms into the discharge. An *in situ* laser calibration of this pixel showed in steady state showed a temperature rise of 4°C for an incident power of 9 mW.

V. SUMMARY

We have tested an infrared imaging bolometer on the CHS plasma, and have proven that the basic idea is workable

on an actual plasma. There are several refinements (rejection of ECH heating, better *in situ* characterization of pixel sensitivities and associated decay times, reduction of stray IR reflections) that we need to implement to allow simpler interpretation of bolometric images. The observed performance with the Agema infrared camera ($\sim 1 \text{ mW/cm}^2$ sensitivity limit for 100 Hz averaging time) can be improved a factor of $4\times$ by switching to our more sensitive Amber Radiance 1 camera. By comparison, the PTS bolometers in use on LHD perform at $\sim 30 \mu\text{W/cm}^2$ sensitivity limit for 100 Hz averaging times. We are proceeding to field an improved IR imaging bolometer on the LHD plasma in 1999.

ACKNOWLEDGMENTS

The authors wish to acknowledge the help of Hank Alvestad, Corky Thorne, Professor K. Matsuoka, and the entire CHS Team. They also thank Dr. Norman Elliott from MST-7 at LANL for providing surface characterization measurements. This work is supported by U.S. DOE Contract No. W-7405-ENG-36 and Monbusho, under auspices of the U.S./Japan Fusion Collaboration Agreement.

¹J. Shivell, G. Renda, J. Lowrance, and H. Hsuan, *Rev. Sci. Instrum.* **53**, 1527 (1982); E. R. Mueller and F. Mast, *J. Appl. Phys.* **55**, 2635 (1984); G. Miller, J. C. Ingraham, and L. S. Schrank, *Rev. Sci. Instrum.* **53**, 1410 (1982).

²K. F. Mast and H. Krause, *Rev. Sci. Instrum.* **56**, 969 (1985).

³D. V. Orlinskij and G. Magyar, *Nucl. Fusion* **28**, 665 (1988).

⁴TFR Group (presented by A. L. Pacquet), *J. Nucl. Mater.* **93&94**, 377 (1980); J. C. Ingraham and G. Miller, *Rev. Sci. Instrum.* **54**, 673 (1983).

⁵G. A. Wurden, B. J. Peterson, and S. Sudo, *Rev. Sci. Instrum.* **68**, 766 (1997).

⁶G. A. Wurden and B. J. Peterson, in *Diagnostics for Experimental Thermonuclear Fusion Reactors 2*, edited by P. Stoff, G. Gorini, P. Prandoni, and E. Sindoni (Plenum, New York, 1998), p. 399–408.

⁷K. Nishimura *et al.*, *Fusion Technol.* **17**, 86 (1990).

⁸B. J. Peterson, S. Sudo, and the CHS Group, *J. Plasma Fusion Res.* **1**, 382 (1998); 8th International Toki Conference Proceedings, 29 Sept.–3 Oct., 1997.